Proc. Natl. Acad. Sci. USA
Vol. 78, No. 12, pp. 7276–7280, December 1981
Biochemistry

Localization of the puromycin binding site on the large ribosomal subunit of *Escherichia coli* by immunoelectron microscopy

(ribosome topography/peptidyl transferase center/IgG antibodies against minor nucleosides/antibiotics)

REINHARD LÜHRMANN, ROLF BALD, MARINA STÖFFLER-MEILICKE, AND GEORG STÖFFLER*

Max-Planck-Institut für Molekulare Genetik, Abteilung Wittmann, D-1000 Berlin-Dahlem, Federal Republic of Germany

Contributed by Wolfgang Beermann, July 2, 1981

ABSTRACT **By using immunoelectron microscopy, we have localized the binding site on 50S *Escherichia coli* ribosomal subunits for puromycin, an antibiotic that interacts with the ribosomal peptidyltransferase center. This was achieved by affinity-labeling 50S subunits with *N*-bromoacetyl puromycin and treating the labeled subunits with an antibody specific for the N^6,N^6-dimethyladenosine moiety of puromycin. The position of the puromycin binding site was then revealed by localizing the attachment sites of the IgG molecules on the surfaces of the 50S subunits under the electron microscope: it was located at the interface between the subunits, on and around the wider lateral protuberance of the 50S subunit. This localizes directly the peptidyl transferase center on the surface of the large ribosomal subunit.**

Puromycin inhibits protein synthesis by substituting for the incoming coded aminoacyl-tRNA and serving as an acceptor for the nascent peptide chain of ribosome-bound peptidyl-tRNA (1). This results in premature release of incomplete polypeptides. The mode of action of puromycin is well understood. The antibiotic is an analogue of the 3′-terminal end of aminoacyl-tRNA and therefore interacts with the acceptor site of the peptidyl transferase center on the large ribosomal subunit. Determination of the puromycin binding site on 50S ribosomal subunits would thus also determine the location of the ribosomal peptidyl transferase center.

We describe here experiments designed to locate this functional region by immunoelectron microscopy, using an antibody against puromycin. Because of the low affinity of puromycin for its ribosomal binding site (2), the antibiotic was bound covalently to 50S subunits, using *N*-bromoacetyl puromycin (the bromoacetyl group is bound to the nitrogen that mimics the α-NH_2 nitrogen of the aminoacyl-tRNA) as an affinity label for the peptidyl transferase center.

MATERIALS AND METHODS

Antiserum against N^6,N^6-dimethyladenosine conjugated to bovine serum albumin (3) was raised in rabbits. The synthesis of N^6,N^6-dimethyladenosine (4), the preparation of immunogens, the immunization procedure, the characterization of the antiserum, and the purification of IgG used in this investigation have been described elsewhere (5). In brief, IgG was purified from immune and preimmune sera by precipitation with ammonium sulfate at 0–40% saturation followed by filtration on Sephadex G-150 columns and affinity chromatography on protein A-Sepharose. The immune IgG reacted with [^{3}H]puromycin, with N^6,N^6-dimethyladenosine, and with 50S ribosomal subunits but only after affinity labeling with *N*-bromoacetyl puromycin. [^{3}H]Puromycin (specific activity, 4000 Ci/mol; 1 Ci = 3.7×10^{10} becquerels) and [^{3}H]bromoacetic acid (specific activity, 75 Ci/mol) were from Amersham/Buchler (Braunschweig, Fed. Repub. of Germany). *Escherichia coli* cells (strain MRE 600) were from the Public Health Laboratory Service, CAMR, (Porton, U.K.).

Ribosomes. 70S ribosomal tight couples from *E. coli* MRE 600 were isolated as described (6). 50S and 30S ribosomal subunits were prepared by zonal centrifugation (7) and, after separation, were concentrated by high speed centrifugation (6).

Affinity Labeling of 50S Subunits. *N*-Bromo[^{3}H]acetyl puromycin (specific activity, 20 Ci/mol) was synthesized as described (8). Two nanomoles of heat-reactivated 50S subunits (6) was incubated at 37°C with 100 nmol of *N*-bromo[^{3}H]acetyl puromycin in 2 ml of buffer I (10 mM $Mg(OAc)_2$/100 mM NH_4Cl/20 mM Hepes, pH 7.4). The reaction was terminated after 2 hr by adding 2-mercaptoethanol to a final concentration of 10 mM. Excess puromycin analogue was removed by centrifuging the reaction mixture through 2 ml of 10% sucrose in buffer I in a Beckman 50 Ti rotor for 4 hr at 45,000 rpm. The ribosome pellet was dissolved in 500 μl of buffer I, and the subunits were dialyzed against 500 ml of buffer I/5 mM 2-mercaptoethanol (three times, 3 hr each). The amount of *N*-bromo[^{3}H]acetyl puromycin that had reacted with 50S ribosomes was determined by measuring the radioactivity; 1100 dpm, 2.8 A_{260} 50S subunits. The yield of covalently bound puromycin was 25% based on 50S subunits.

Electron Microscopy. Samples for electron microscopy were taken from the sucrose gradients as indicated in Fig. 1. The samples were placed on grids by using the double-layer carbon technique (9), and the specimens were negatively contrasted with 0.5% uranyl acetate. Photographs were taken at instrumental magnifications of 71,000 or 110,000 in a Philips EM 301 operated at 80 kV.

RESULTS

Affinity Labeling of 50S Ribosomal Subunits with *N*-Bromoacetyl Puromycin and Reaction with Antibody. 50S ribosomal subunits were incubated with *N*-bromo[^{3}H]acetyl puromycin, resulting in 25% labeling.

For localization of the puromycin binding site, we used IgG specific for the dimethyladenosine moiety of the antibiotic. Affinity-labeled 50S subunits were treated with antibody and subjected to sucrose density gradient centrifugation to separate the ribosome–IgG complexes from the unreacted 50S subunits and excess antibody. In the presence of specific antibody, a shoulder was obtained that sedimented faster than the 50S subunits and amounted to 15% of the total 50S subunits at the optimal antibody concentration (Fig. 1*a*). The ribosome-bound puromycin residue was thus available for antibody binding on at least 60% of the affinity-labeled subunits. Such 50S sub-

The publication costs of this article were defrayed in part by page charge payment. This article must therefore be hereby marked "*advertisement*" in accordance with 18 U. S. C. §1734 solely to indicate this fact.

* To whom reprint requests should be addressed.

unit–antibody complexes were formed only when affinity-labeled 50S subunits were incubated with antibody against puromycin; they were not formed in control experiments using [^{3}H]puromycin instead of the affinity analogue (Fig. 1*b*) or IgG prepared from a pre-immune serum (Fig. 1*c*).

Electron Microscopy of Affinity-Labeled 50S Subunit–Antibody Complexes. The dimer peak from the sucrose density gradient shown in Fig. 1*a* was used for specimen preparation. A typical electron micrograph (Fig. 2*a*) shows 50S subunits without bound antibody molecules and two types of subunit–antibody complexes. One type, represented by two examples, consists of subunit pairs joined by an IgG (dimers); the other type (three examples) consists of monomeric 50S subunits, each having a single IgG molecule bound (monomers). Quasisymmetric crown-shaped 50S subunits were predominant; asymmetric kidney-shaped subunits were rare. The shapes, dimensions, and adsorption behavior of puromycin-labeled 50S subunits were indistinguishable from those of unmodified 50S particles.

Examples of antibody-dimerized subunits in which both subunits assume the crown-shaped image are shown in Fig. 2 *b* and *c*. The subunits in each pair are related by a rotation of 90°–180° about a vertical axis. In 95% of the interpretable 50S–antibody complexes, the Fab arms of the connecting antibody molecules were bound to a region on the 50S particle located around the wider lateral protuberance opposite the rod-like appendage (Fig. 2 *b* and *c*; see Fig. 3*a* for nomenclature). The same binding site was deduced from monomeric 50S subunits with a single attached antibody molecule (Fig. 2*d*). The apparent area of contact between the antibody and the crown-shaped 50S subunits is illustrated by drawings (Fig. 2 *b6–e6*; Fig. 3*b1*). Antibody binding to kidney-shaped 50S subunits was observed in ≈5% of the subunit–antibody complexes evaluated, and here the antibody was bound to the concave side of the subunit; the points of binding of the Fab arms were in a region extending from the base of the notch toward the blunted end (Fig. 2 *e* and *f*). Evaluation of the kidney-shaped 50S subunits having bound IgG molecules made it possible to propose a single site for the antibody binding region (Fig. 3*b2*).

Dimers joined simultaneously by two antibodies and aggregates of ribosome–antibody complexes with three or more 50S subunits linked by several IgG molecules were not observed. The lack of such complexes confirms that the puromycin analogue was bound to a single site.

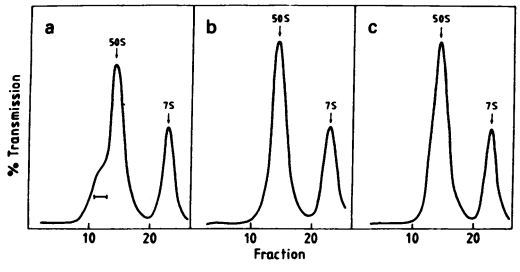

FIG. 1. Dimerization of affinity-labeled 50S subunits with puromycin-specific antibody. Two A_{260} units of 50S ribosomal subunits were incubated with IgG in 200 μl of 5 mM $Mg(OAc)_2$/100 mM NH_4Cl/20 mM Hepes, pH 7.4, for 5 min at 37°C and then kept on ice for 30 min. The reaction mixture was layered onto sucrose density gradients [10–30% sucrose in 50 mM Tris·HCl, pH 7.5/100 mM NH_4Cl/5 mM $Mg(OAc)_2$] and centrifuged in an SW40 rotor for 14 hr at 20,000 rpm. The sedimentation profiles were determined by continuously monitoring the transmission at 260 nm; 500-μl fractions were collected. The direction of sedimentation is from right to left. (*A*) Affinity-labeled 50S subunits preincubated with 1.5 A_{280} units of IgG specific for N^6,N^6-dimethyladenosine. ⊢, Fractions used for specimen preparations. (*B*) [^{3}H]Puromycin-labeled 50S subunits preincubated with 1.5 A_{280} units of IgG specific for N^6,N^6-dimethyladenosine. (*C*) Affinity-labeled 50S subunits, preincubated with 1.5 A_{280} units IgG from pre-immune serum. Note that the electron micrographs prepared from the 50S peak in *b* and *c* did not show any subunit–antibody complexes.

Three-Dimensional Location of the Puromycin Binding Site. This requires the determination of the antibody binding site on crown-shaped and on kidney-shaped 50S subunits. From Fig. 2, the puromycin binding site on 50S subunits appears to be in an area between the central protuberance and the wider lateral protuberance but closer to the latter (Fig. 3*c*). The rod-like appendage is separated from the puromycin binding site by ≈200 Å (Fig. 3*c*).

The localization of the antibody binding site on the kidney-shaped subunits (Fig. 2 *e* and *f*; Fig. 3*b2*) allows the further conclusion that the puromycin binding site is located at the interface between the 50S and the 30S subunits since the concave side of the 50S subunit bearing the notch faces the 30S subunit in each of the proposed 70S models (9–15).

Independent of antibody-labeling studies, it has been suggested (9–15) that the wider lateral protuberance in the crown-shaped subunits (position 3 in Fig. 3*a1*) and the bulge between the notch and the blunted end in the kidney-shaped subunits (Fig. 3*a2*, position 6) corresponds to one and the same area in the three-dimensional model of the 50S subunit (see Fig. 3*c*).

This assumption is supported by the observation of subunit dimers in which the antibody connects a crown-shaped particle with a kidney-shaped subunit (Fig. 2*f*). These subunit–antibody complexes are of particular importance for the three-dimensional localization of the antibody binding site, because they show that two sites, apparently different when seen on two-dimensional electron micrographs, correspond to a single site in the three-dimensional structure.

The puromycin binding site and thus the peptidyl transferase center have been located on a distinctive structural feature of the 50S subunit (16, 17). This area is also well defined on the three-dimensional models of the 50S subunit proposed by Lake (11) and by Boublik *et al.* (12). Because the electron micrographs of negatively contrasted 50S subunits published by these workers are similar to those described here, we have attempted to project the puromycin binding site onto the three-dimensional 50S subunit models proposed by them.

In the 50S model of Boublik *et al.* (12), the puromycin binding site can be located near the smaller "right" crest (Fig. 3*d*) by assuming that the more elongated side crest corresponds to the stalk described by Lake (11) and Stöffler *et al.* (14–16).

In the case of the model of the 50S subunit proposed by Lake (11), the puromycin binding site would be located on or in the vicinity of the one lateral protuberance, which is shorter, blunter, and wider than the rod-like appendage (Fig. 3*e*). It is noteworthy that this area is in a region that has been proposed as location of the peptidyl transferase center on the basis of an indirect approach (18).

DISCUSSION

Our study of the location of the puromycin binding site on 50S ribosomal subunits showed a single antibody binding site located on one of the most distinctive structural features of the 50S subunits (see Fig. 3). The low frequency of aberrant antibody attachment sites (≈5%) and their location at the lower pole of the subunit (i.e., in a region in which an unspecific interaction via the Fc part of the molecule was occasionally observed) made it unnecessary to take this second site into consideration.

The validity of our study depends on several experimental variables. One is the specificity of the antibody preparation for

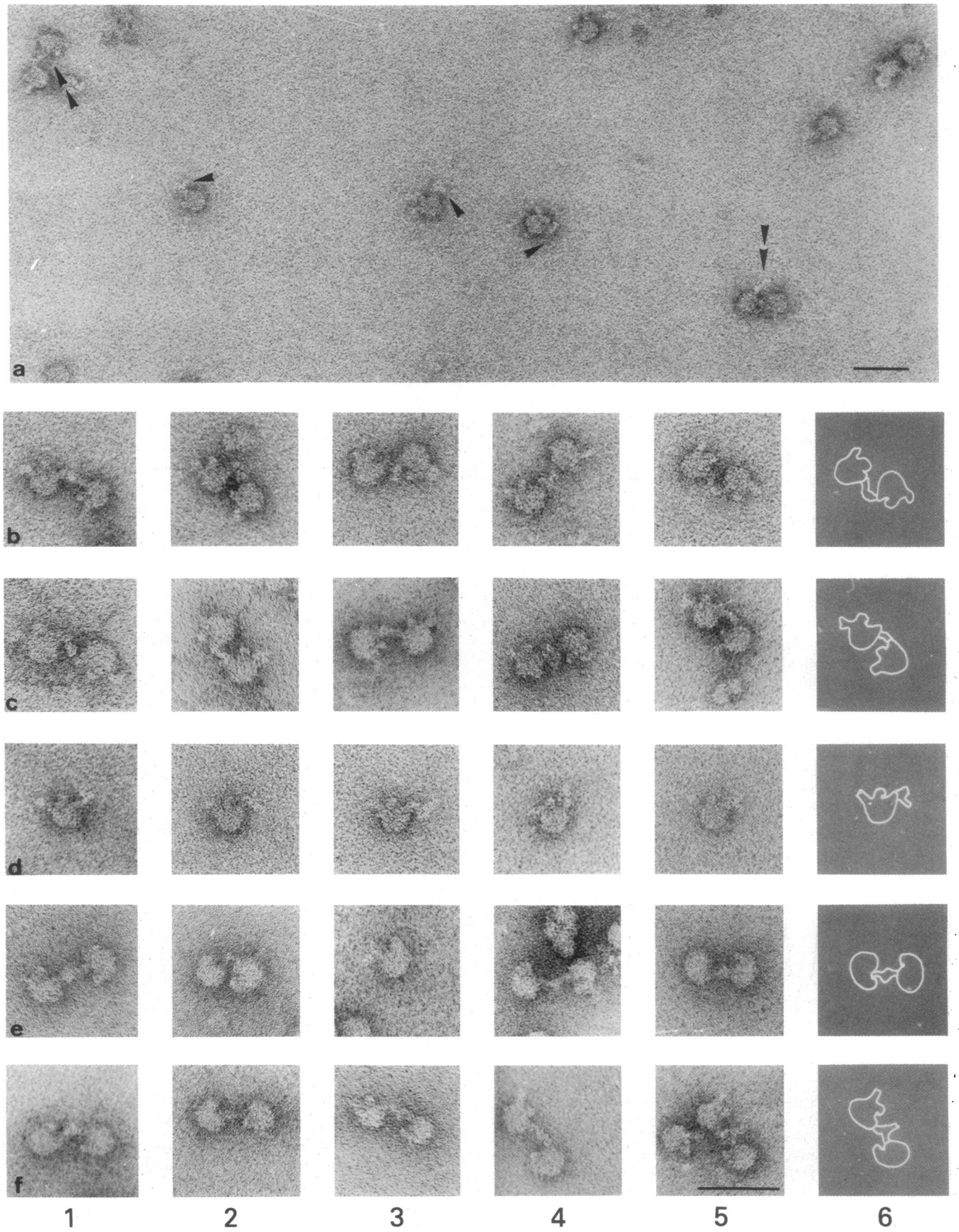

FIG. 2. Electron micrographs of puromycin-labeled 50S subunits treated with IgG specific for N^6,N^6-dimethyladenosine. (*a*) General field. ►, 50S·IgG complexes; ►►, 50S·IgG·50S complexes. (*b–f*) Selected fields of antibody-linked subunit dimers (*b* and *c*) and monomers (*d*), showing the ribosomal subunits in crown-shaped projections; antibody–subunit complexes, showing kidney-shaped projections (*e*); and crown-shaped particles connected with kidney-shaped particles (*f*). (*b6–f6*) Interpretative drawings corresponding to *b5–f5*. From total of 221 50S subunits having bound antibody molecules, 12 showed aberrant antibody binding, predominantly to the lower pole of the 50S particle. The antibody binding site on the

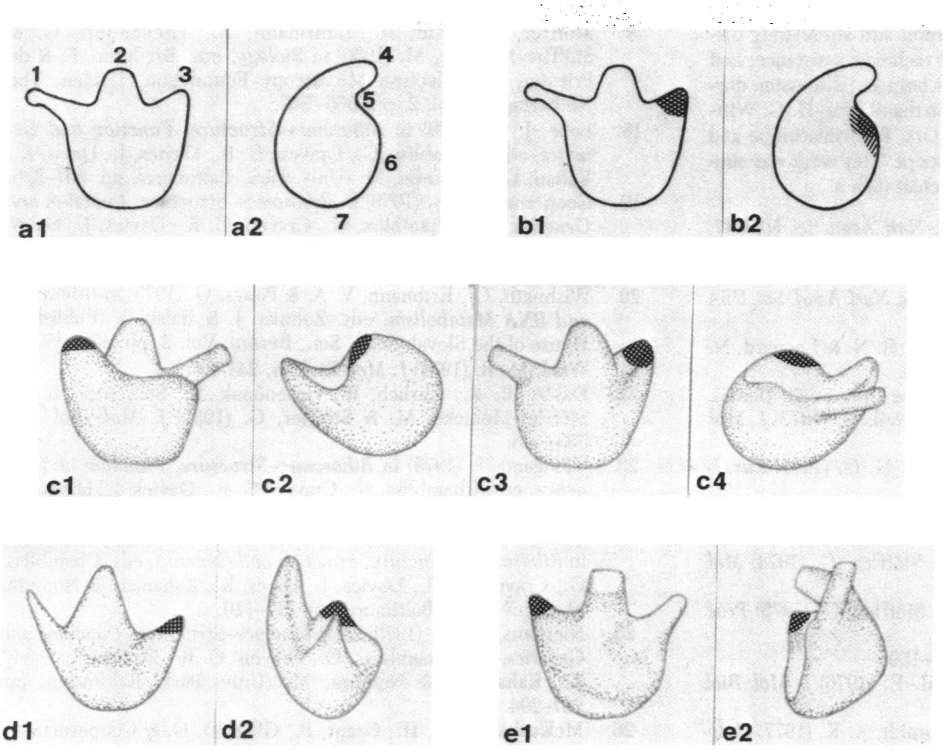

FIG. 3. Localization of the puromycin binding site. (*a1* and *a2*) Typical structural features of 50S ribosomal subunits in the crown-shaped and the kidney-shaped, respectively, projections: 1, Rod-like appendage; 2, central protuberance; 3, wider lateral protuberance; 4, pointed end; 5, notch; 6, bulge; 7, blunted end. (*b1* and *b2*) Two-dimensional localization of the antibody binding site (■) on crown-shaped and kidney-shaped, respectively, projections. Three-dimensional localization of the puromycin binding site on the 50S model proposed by Tischendorf *et al.* (10) with modifications described by Stöffler and Stöffler-Meilicke (27) (*c*) by Boublik *et al.* (12) (*d*) and by Lake (11) (*e*). The location of the puromycin binding site on the models of Boublik and of Lake represents an attempt to interpret our location in terms of the three-dimensional subunit models.

the antibiotic to be localized. This specificity was demonstrated by showing that the antibodies reacted with puromycin, or with the puromycin analogue in the free state, or associated with ribosomes but not with unlabeled 50S ribosomal subunits.

Demonstration of the specificity of the affinity label used in such a study is also of great importance.

Evidence must be provided that the labeling occurred in a site-specific manner, and the identities of labeled ribosomal components must be convincingly established. Of the several affinity analogues of puromycin (see ref. 19), the *N*-bromoacetyl derivative fulfils these criteria best for several reasons. (*i*) Several electrophoretic and immunological methods have been used for the identification of the protein labeled by *N*-bromoacetyl puromycin; it is principally proteins L1, L2, L23, and L27 that react with the puromycin analogue (unpublished results). (*ii*) Previous studies have shown that covalently bound *N*-iodoacetyl puromycin inhibits the binding of C-A-C-C-A-LeuAc to labeled 50S subunits, suggesting a P-site labeling process (20). The fact that the puromycin analogue bound at a single distinct topographical site on 50S ribosomal subunits (see Figs. 2 and 3) rather than to various sites scattered over the surface of the 50S subunit further indicated that the labeling was specific. A variety of other data support our notion that we have located the peptidyl transferase center, although the resolution does not suffice to distinguish A and P sites at this point. The puromycin binding site reported here is near the ribosomal binding site for another peptidyl transferase inhibitor, chloramphenicol, which has been determined by electron microscopy of immunoprecipitates with an amphenicol-specific antibody (16, 17).

The locations of the four proteins labeled with *N*-bromoacetyl puromycin (L1, L2, L23, and L27) have been determined with protein-specific antibodies. Protein L1, protein L2, protein L23, and protein L27 all have antigenic determinants exposed in an area near the puromycin binding site (10, 16, 18, 21, 22). Moreover, each of these proteins is implicated in other affinity-labeling studies of peptidyl transferase (19, 23) and is among the crosslinks between "peptidyl transferase proteins" (24). Protein L2 is also one of the five proteins essential for peptidyl transferase activity as judged from reconstitution experiments (25). Other studies have led to the identification of other proteins, (i.e., L11, L16, and L18) at or near the peptidyl transferase center (cf. refs. 19, 23, and 25). Of these, L16 and L18 have also been located relatively close to the puromycin site reported here; for L11, the correspondence is less satisfactory (16).

The localization of a reaction site of puromycin with 30S subunits, by using immunoelectron microscopy, has recently been reported (26). This site was mapped on the top of the head of the small subunit. Although the functional significance of this binding site has not been established, it has been pointed out that such a site may be a part of a common puromycin affinity site in 70S ribosomes. This site, is, however, quite remote from the peptidyl transferase center in the 70S models proposed by Lake (18) and by us (14, 15, 27).

The decoding region on the 30S ribosomal subunit has been found at a distinctive structural feature of the small subunit by several investigators (for review, see ref. 27). The puromycin binding site deduced from two-dimensional electron micrographs of 50S subunits is sufficiently well defined to allow a tentative three-dimensional localization on each of the three 50S subunit models so far proposed (Fig. 3 *c–e*) and also allows deductions as to the location of the peptidyl transferase center on the 50S ribosome. Combining these sets of data would, in principle, suffice for the construction of a model of the arrangement of tRNAs in the functioning ribosome. Indeed, proposals as to the arrangement of mRNA and tRNA in the monomeric ribosome have been made (16, 18, 23, 27). However, these models require that the structures of the ribosomal subunits be elucidated. This question has been approached by three-dimensional image reconstruction of single negatively contrasted ribosomal particles (28) and of crystals of ribosomal subunits (29).

kidney-shaped subunits was further substantiated by electron micrographs of ethanol-precipitated 50S subunits treated with the puromycin analogue, which showed kidney-shaped subunits more frequently (16). Bars = 50 nm.

We thank Dr. Paul Woolley for many helpful and stimulating discussions; R. Ehrlich and S. Rothe for expert technical assistance; and B. Kastner, R. Hasenbank, and K.-H. Rak for help and discussion during the preparation of the manuscript. We also thank Prof. H. G. Wittmann for constant interest and support and Drs. R. Brimacombe and E. R. Dabbs for critically reading the manuscript. This work was supported by the Deutsche Forschungsgemeinschaft (Sfb 9).

1. Nathans, D. & Lipmann, F. (1961) *Proc. Natl. Acad. Sci. USA* **47**, 497–504.
2. Pestka, S. (1974) *Methods Enzymol.* **30**, 261–282.
3. Erlanger, B. F. & Beiser, S. M. (1974) *Proc. Natl. Acad. Sci. USA* **52**, 68–74.
4. Townsend, L. B., Robins, R. K., Loeppka, R. N. & Leonard, N. J. (1964) *J. Am. Chem. Soc.* **86**, 5320–5325.
5. Dieckhoff, J. (1980) Dissertation (Technische Universität, Berlin).
6. Noll, M., Hapke, B., Schreier, M. H. & Noll, H. (1973) *J. Mol. Biol.* **75**, 281–294.
7. Hindennach, I., Stöffler, G. & Wittmann, H. G. (1971) *Eur. J. Biochem.* **23**, 7–12.
8. Pongs, O., Bald, R., Wagner, T. & Erdmann, V. A. (1973) *FEBS Lett.* **35**, 137–140.
9. Tischendorf, G. W., Zeichhardt, H. & Stöffler, G. (1974) *Mol. Gen. Genet.* **134**, 187–208.
10. Tischendorf, G. W., Zeichhardt, H. & Stöffler, G. (1975) *Proc. Natl. Acad. Sci. USA* **72**, 4820–4824.
11. Lake, J. A. (1976) *J. Mol. Biol.* **105**, 131–159.
12. Boublik, M., Hellmann, W. & Roth, H. E. (1976) *J. Mol. Biol.* **107**, 479–490.
13. Boublik, M., Hellmann, W. & Kleinschmidt, A. K. (1977) *Cytobiologie* **14**, 293–300.
14. Kastner, B., Stöffler-Meilicke, M. & Stöffler, G. (1980) in *Biology*, eds. Brederoo, P. & de Priester, W. (Electron Microscopy Foundation, Leiden, The Netherlands), Vol. 2, pp. 564–565.
15. Kastner, B., Stöffler-Meilicke, M. & Stöffler, G. (1981) *Proc. Natl. Acad. Sci. USA* **78**, pp. 6652–6656.
16. Stöffler, G., Bald, R., Kastner, B., Lührmann, R., Stöffler-Meilicke, M., Tischendorf, G. & Tesche, B. (1979) in *Ribosomes–Structure, Function and Genetics*, eds. Chambliss, G., Craven, G. R., Davies, J., Davis, K., Kahan, L. & Nomura, M. (Univ. Park, Baltimore), pp. 171–205.
17. Stöffler, G., Bald, R., Lührmann, R., Tischendorf, G. & Stöffler-Meilicke, M. (1980) in *Biology*, eds. Brederoo, P. & de Priester, W. (Electron Microscopy Foundation, Leiden, The Netherlands), Vol. 2, pp. 566–567.
18. Lake, J. A. (1979) in *Ribosomes–Structure, Function and Genetics*, eds. Chambliss, G., Craven, G. R., Davies, J., Davis, K., Kahan, L. & Nomura, M. (Univ. Park, Baltimore), pp. 207–236.
19. Cooperman, B. S. (1979) in *Ribosomes–Structure, Function and Genetics*, eds. Chambliss, G., Craven, G. R., Davies, J., Davis, K., Kahan, L. & Nomura, M. (Univ. Park, Baltimore), pp. 531–554.
20. Wishnath, G., Erdmann, V. A. & Pongs, O. (1975) in *Ribosomes and RNA Metabolism*, eds. Zelinka, J. & Balan, J. (Publishing House of the Slovak Acad. Sci., Berlin), Vol. 2, pp. 439–450.
21. Wabl, M. R. (1974) *J. Mol. Biol.* **84**, 241–247.
22. Dabbs, E. R., Ehrlich, R., Hasenbank, R., Schroeter, B.-H., Stöffler-Meilicke, M. & Stöffler, G. (1981) *J. Mol. Biol.* **149**, 553–578.
23. Ofengand, J. (1979) in *Ribosomes–Structure, Function and Genetics*, eds. Chambliss, G., Craven, G. R., Davies, J., Davis, K., Kahan, L. & Nomura, M. (Univ. Park, Baltimore), pp. 497–529.
24. Traut, R. R., Lambert, J. M., Boileau, G. & Kenny, J. W. (1979) in *Ribosomes–Structure, Function and Genetics*, eds. Chambliss, G., Craven, G. R., Davies, J., Davis, K., Kahan, L. & Nomura, M. (Univ. Park, Baltimore), pp. 89–110.
25. Nierhaus, K. H. (1979) in *Ribosomes–Structure, Function and Genetics*, eds. Chambliss, G., Craven, G. R., Davies, J., Davis, K., Kahan, L. & Nomura, M. (Univ. Park, Baltimore), pp. 267–294.
26. McKuskie Olson, H., Grant, P., Glitz, D. G. & Cooperman, B. S. (1980) *Proc. Natl. Acad. Sci. USA* **77**, 890–894.
27. Stöffler, G. & Stöffler-Meilicke, M. (1981) in *International Cell Biology 1980–1981*, ed. Schweiger, H. G. (Springer, Berlin), pp. 93–102.
28. Knauer, V. & Hoppe, W. (1980) in *Biology*, eds. Brederoo, P. & de Priester, W. (Electron Microscopy Foundation, Leiden, The Netherlands), Vol. 2, pp. 702–703.
29. Yonath, A. E., Müssig, J., Tesche, B., Lorenz, S., Erdmann, V. A. & Wittmann, H. G. (1980) *Biochem. Int.* **1**, 428–435.